# STRAIN ANALYSIS DURING THE SYMMETRIC AND ASYMMETRIC ROLLING OF 7075 Al ALLOY SHEETS

C. Q. Ma, L. G. Hou, J. S Zhang, L. Z. Zhuang

State Key Laboratory for Advanced Metals and Materials, University of Science and Technology Beijing, 30 Xueyuan Rd.; Haidian district, 100083, PR China

## Abstract

The strain components (shear strain, strain in rolling direction), equivalent strain and deformation of elements through sheet thickness in symmetric / asymmetric rolled AA 7075 Al alloy sheets were quantified using finite element method (FEM) with taking into account the deformation histories. The FEM results showed that positive and negative shear strains can be formed after a single-pass rolling and the total shear strain in the middle thickness of asymmetric rolled sheet (asymmetric ratio: 1.25) can be greatly increased compared to that of symmetric rolled sheet for the introduction of severe plastic shear deformation, so as to improve the equivalent strain. Using the engraved-mark experimental method the FEM results were verified to be consistent. Moreover, it can be found that much more shear bands will be introduced through the thickness of asymmetric rolled sheet, especially in the middle layer, indicating that asymmetric rolling greatly favors to through-thickness deformation accumulation.

## Introduction

Asymmetric rolling (ASR) can induce larger shear strain and increase the through-thickness uniformity of the shear deformation for alloy sheets. Compression deformation appeared in symmetric rolling process also can be performed with redundant shear deformation under ASR condition. Mostly the shear deformation can play a critical role in the grain refinement of metallic materials as well as improving their mechanical properties [1]. Experimental investigations about the effect of ASR on the grain refinement and mechnaical properties were done for pure metals and some alloys [2-11]. These studies showed that the microstructures of ASR processed metals were refined to less than 10 μm or even to nano size, and the formability and mechnacial properties of the metals were improved significantly. They found that two kinds of shear bands produced by shear defromation were intersected with each other [10, 12], inducing the break or refinement of large elongated grains. Therefore, the analysis of shear strain during rolling process is particularly improtant, and some studies used Finite element (FE) simulations to analyze the through-thickness strain distribution of ASR processed sheets [13, 14]. However, the strains achieved in these studies does not exhibit exact values because the direction of shear stress and shear strian in a roll bite will be changed to opposite directions before and after a neutral plane [15]. In order to clarify the effect of shear strain on the microsstructure evolution during ASR processing, it is essential to quantitatively understand the deformation behaviors in the ASR rolled sheet.

This study aims to quantidy the strains in each component as well as the equivalent strain during multi-pass ASR processing with different asymmetric ratios (i) using FE simulation. And the ASR experiments with different asymmetric ratios were also carried out. By tracking the shape of the reference marks engraved artificially on the sheet side after per-pass rolling, the deformation was obtained and analyzed. Also introducing large shear strain through the thickness of ASR processed sheet were verified through the engraved-mark method.

## Methods of analysis

### Experimental procedures

The 7075 Al alloy sheets with size 20 mm x 40 mm x 150 mm were treated at 400 oC for 1 h to achieve homogeneous temperature. Also some engraved-marks were made on the longitude section (Rolling direction-Normal direction (RD-ND) plane) that were used to evaluate and observe directly the sheet deformation after symmetric and asymmetric rolling (as shown in Fig.1). The asymmetry was introduced by using same rotational speeds (3.75 rev/min) but different roll diameters of the upper and lower rolls. Three asymmetric ratios applied were: 1:1.00 (φ300:φ300, named symmetric rolling, noted as SR), 1:1.12 (φ170:φ190, noted as ASR-1.12) and 1:1.25 (φ160:φ200, noted as ASR-1.25). Here, for ASR the lower roll was the lager roll. No lubricant was applied during the rolling process. All sheets were rolled to the final thickness of 8 mm with 4 passes, corresponding to 60 % thickness reduction. The sheets were rotated 180o along the transverse direction (TD) axes in the adjacent two passes to decrease the accumulation of curvature.

### FEM simulation

For getting much more information about plastic deformation and to further understand the strain distribution during ASR and SR processing, an elastic-plastic thermo-mechanical coupled FE model with explicit dynamic analysis was used. The rolling model was set using MSC.MARC code. The workpiece and rolls were assumed to be elastic-plastic materials and perfect rigid bodies, respectively. Considering the spread of sheets in width might be very small, the deformation occurred in the sheets during rolling was treated as a plane-strain deformation that can be described on the plane consisting of the rolling and thickness directions [13].

To ensure the accuracy of hot rolling simulation, heat transfer and heat generation were also taken into account. Heat generation can be mainly induced by plastic deformation and friction between the rolls and workpieces, and the transfer coefficients were set as 0.95 and 1, respectively. The conduct heat transfer coefficient between the rolls and workpieces was set as 30

Kw/m$^2\cdot$°C [16]. A coulomb friction model was applied to describe the friction behaviors between rolls and workpieces. The friction coefficient, μ, was adjusted by a series of combined experimental tests and FEM simulations and 0.35 was used. The flow stress curves of 7075 Al alloy at different strain rates (0.05 s$^{-1}$, 0.5 s$^{-1}$, 5 s$^{-1}$) and different temperatures (250 °C, 300 °C, 350 °C, 400 °C, 450 °C) were obtained from ref. [17]. It was assumed that there were guides after the roll stand, which can prevent the sheet from bending and lead sheet into the next roll gap. The schedule of multi-pass rolling simulation was same to the experiments.

## Results and discussion

Fig.1 supplies a first outlook of engraved-marks produced after the 4th rolling pass under symmetric and asymmetric (ASR-1.25) conditions. The different profiles of marks generated at the roll gap by the two rolling conditions become clear after rolling. It is apparent that during ASR, the marks are not asymmetry with respect to the center plane of sheets compared with that after SR. Marks that are perpendicular to the rolling plane before rolling tend to incline towards the rolling direction and were stretched to almost 22 mm and 3 mm along rolling direction, and shown as "S"and "C" shapes after asymmetric and symmetric rolling, respectively.

In addition, the accuracy of FEM simulation was also verificated through the profile of reference, the shear angles, (θ / °, defined as the angle between the marks before and after rolling) obtained by FEM simulation and experiment, are 60.13 ° and 61.8 °, respectively, as shown in Fig.1 (b). The error is less than 3 %.
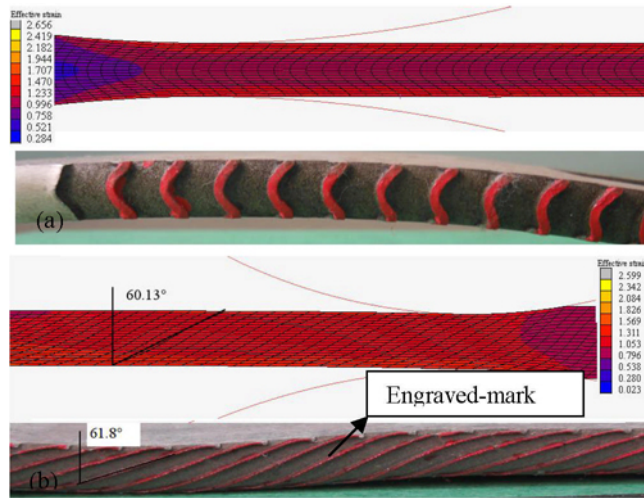


Figure 1. FEM and experimental profiles of engraved-marks after 4-pass SR (a) and ASR-1.25 (b) processing.

Fig.2 (a) shows the deformed meshes after SR and ASR processing, corresponding to the engraved-marks shown in Fig.1. It should be noted that the profile of elements produced by ASR is not symmetric with respect to the center plane of sheet, which is completely different from that induced by SR. This is consistent with the experimental results and the flection through the thickness becomes larger with increasing asymmetric ratios. The deformation of elements occurred during rolling with different asymmetric ratios can be simplified as depicted in Fig.2 (b). An initial element of 1 mm x 1 mm at the surface layer or center layer is distorted to a parallelogram, in which the width ($l$), height ($h$) and angle (θ) can be calculated through FEM results, as shown in

the right table of Fig.2. The changes of width and height with increasing asymmetric ratios are not large, about 2.45 mm and 0.40 mm, respectively. On the contrary, shear angle is increased along with increasing asymmetric ratios, especially at the center layer the difference of shear angles produced by SR and ASR-1.25 can be up to 56 °, which means there is almost no shear deformation during SR compared with large shear deformation occurred in ASR. But the shear deformation at the surface could be occurred not only in ASR but also in SR processing, which can be mainly induced by friction between the rolls and sheet surfaces. The difference of shear angle between SR and ASR is caused by the redundant shear strain introduced by cross-shear rolling [15], which is a special type of deformation during ASR. In addition, the lengths of elements after rolled with asymmetric ratio of 1.0, 1.12 and 1.25 are 6 mm, 11.7 mm and 16.1 mm, respectively, which also indicates that more deformation in RD and ND can be generated with increasing asymmetric ratios.

Shear and effective strains were always calculated by the embedded-pin method [18-21] based on equations proposed by Cui et al. [19]. But the method did not exhibit the exact strain values, because the effect of reverse shear deformation after the neutral plane (NP) was not considered in these equations [15]. The direction of shear strains will be changed through the NP, and sheets will experience positive and negative shear strains before and after the NP in the roll bite. Shear strains always are increased regardless of its direction, so the total shear strain, γ, should contain both of them, and is expressed as follows[22]:

$$\gamma = \gamma^+ + \left|\gamma^-\right| = \int_0^{t(NP)} \frac{d_{\gamma_{xy}}}{dt} dt + \int_{t(NP)}^{t(steady)} \left|\frac{d_{\gamma_{xy}}}{dt}\right| dt \quad (1)$$

Here, $\gamma^+$ denotes a positive shear strain induced by shear stress before NP and $\gamma^-$ is the negative shear strain induced by shear stress after NP. In other words, the γ represents the total magnitude of shear strains under considering the deformation histories during rolling.

Fig. 3 shows the histories of shear strain at five locations through sheet thickness, i.e., TS, TQ, MT, BQ and BS, as shown in Fig.2 (a), during 1st pass rolling with asymmetric ratio of 1.0 and 1.25, respectively. It can be obviously found that the distribution of shear strain is symmetry to the center plane, and the value of shear strain at MT is almost zero during the whole SR processing (as shown in the Fig.3 (a)). On the contrast, the variation of shear strain is no longer symmetry to the center plane, due to the presence of "shear cross zone", and more shear deformation is induced, promoting the easy penetration of deformation to the middle thickness, as shown in the Fig. 3(b). The shear strain at MT can intensely change the deformation zone during ASR processing. It should be noted that the magnitude of γ at TS (surface closed to the faster roll with larger roll biting geometry ($L_d/t_d$ =1.11, ratio of projected contact length, $L_d$ to average thickness of sheet, $t_d$)) is much larger than that of γ at BS (surface closed to the slower roll with smaller $L_d/t_d$=0.99) during ASR processing, which probably dues to the effect of roll biting geometry on the shear strain distribution. The through-thickness deformation during rolling depends strongly on $L_d/t_d$, and the strain can be increased with increasing $L_d/t_d$[15]. Also, Fig.4 shows that the histories of strain in ND at center elements of rolled sheet with different asymmetric ratios. It can be seen that there is no significant difference in the strain accumulation in ND for SR and ASR, which indicates that the asymmetric rolling main improve the shear strain at the same time there is no reduction in compressive strain in ND.
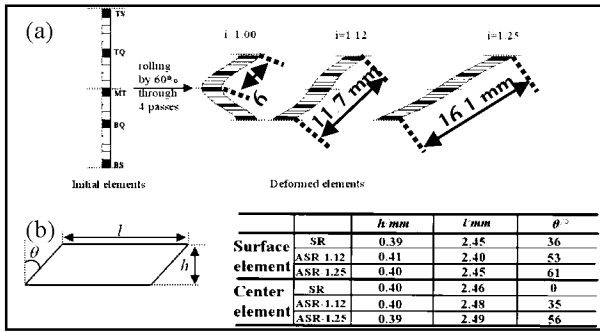
Figure 2. (a) Initial and deformed mesh after rolling with different asymmetric ratios; (b) simplified description of deformed element after rolling and calculated values of parameters (TS and BS: top and bottom surfaces; MT: the element located at the center; TQ and BQ: 1/2 thickness located between center and top or bottom surface.)
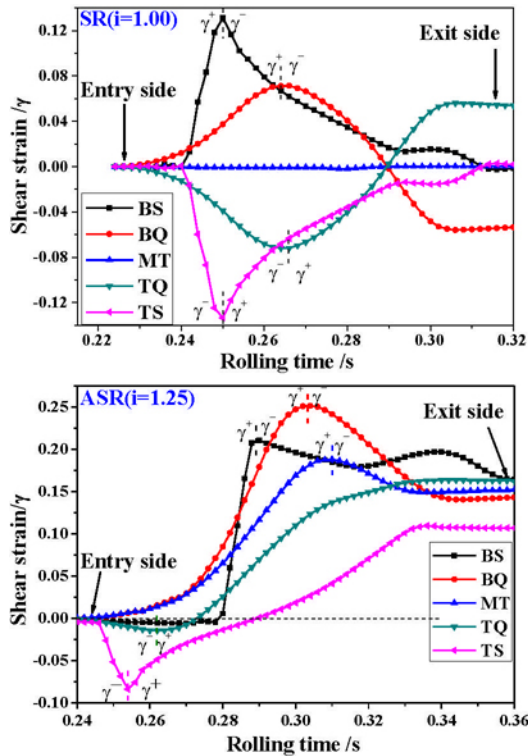


Figure 3. The histories of shear strain at different locations through the thickness of rolled sheets: (a) SR; (b) ASR-1.25

The total shear strain after 4 passes was obtained by calculating the components of every pass, as shown in Fig.5, and it is found that the total shear strain is increased with increasing asymmetric ratios through sheet thickness, but the increment of shear strain at the surfaces is much less than that at center, which means that the uniformity of strain distribution will be improved through sheet thickness. The uniformity improvement is consistent with the experimental results in ref. [11], in which the microstructural distribution was observed to be uniform through thickness of ASR processed sheet as the speed ratios were increased. The magnitude of $\gamma$ at MT is 0.026, 0.52 and 0.836 after 4 passes SR, ASR-1.12 and ASR-1.25 rolling, respectively.

On the other hand, another phenomenon should be noted that the magnitude of shear strain increment from SR to ASR-1.12 (~0.5) is larger than that from ASR-1.12 to ASR-1.25 (~0.31). Also, according to the profile of engraved-mark shown in Fig.1, the shear strain can be calculated using following functions given by [9, 21]

$$\gamma = \frac{2(1-r)^2}{r(2-r)} \tan\theta \ln\frac{1}{1-r} \qquad (2)$$

Where $\theta$ is the shear angle shown in Fig.1, and r is the reduction ratio of the rolling process which is given by

$$r = 1 - \frac{h_1}{h_0} \qquad (3)$$

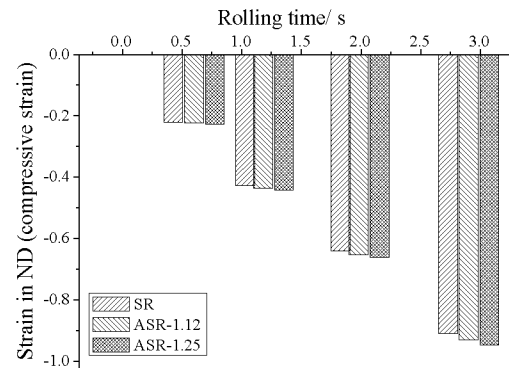Here H and h are the thickness of the sheet before and after rolling, respectively.



Figure 4. The histories of strain in ND at center elements of rolled sheets

The hollow circular symbol shown in Fig.5 (a) is the calculated values through experiment results, and these results indicate that although there are some errors, the FE simulation results are still receivable. In previous studies [9, 15, 22], the strain in the rolling direction, $\varepsilon_{RD}$, is regarded as equal to the minus strain in the normal direction, $\varepsilon_{ND}$. But as shown in Fig.5 (b), $\varepsilon_{ND}$ is larger than $\varepsilon_{RD}$, and with increasing asymmetric ratios, the difference between the strain components is increased. The results may also be explained by the description of Fig.2 (a): the length of deformation bands in RD is increased with asymmetric ratio increasing, which indicates more deformation can be generated.

The microstructures of SR and ASR-1.25 processed sheets (after solution treatment at 470 °C for 1 h) taken from the middle layer of RD-ND plane are shown in Fig.6. Compared with the SR processed sheet with coarse elongated grains, the ASR processed sheet exhibits the presence of refined grains. Because the deformation in ASR processing is not only compression but also much more additional shear deformation, and the grain refinement in ASR processed sheet mainly due to these shear strains [19, 23]. Additional shear deformation can generate more internal shear bands in grains which contain more sub-boundaries, and grain refinement during ASR processing can be resulted from the development of sub-boundaries into high angle boundaries promoted by a simultaneous action of shear deformation [19].
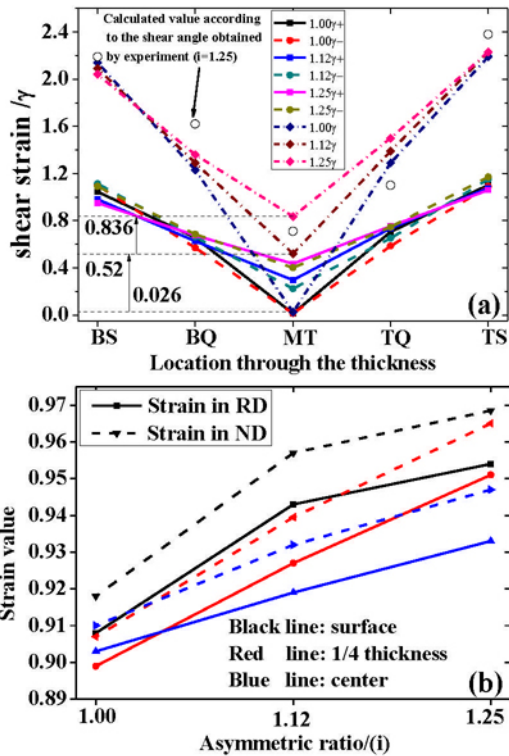
447

Fig.5 Total strains of rolled sheets calculated by FE simulation (full symbols) and experimental (empty symbols) results: (a) shear strain; (b) strains in RD and ND
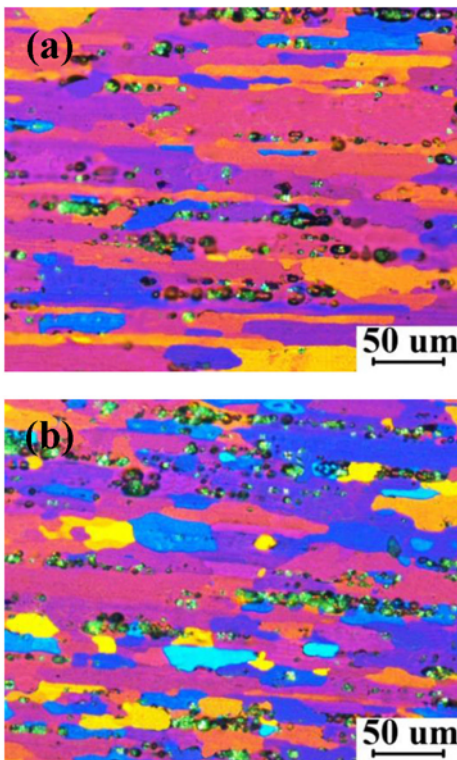


Fig.6 Microstructures of SR (a) and ASR-1.25 (b) processed sheets

## Conclusions

ASR processes with different asymmetric ratios were analyzed by FE simulation and experimental methods in terms of deformation pattern, components of plastic strain, through-thickness strain distribution as well as microstructures with comparing to SR process. The inclination of engraved marks is increased with the asymmetric ratio increasing, especially at the middle layer of processed sheet, the inkling angle is increased from 0° to 61.8° for ASR-1.25 processing. The ASR processed sheets undergo positive and negative shear strains before and after neutral plane during rolling, and with considering these two shear strains the total shear strain at the middle thickness of rolled sheets can be increased with increasing asymmetric ratios. And the experimental results agree well with the FEM results. The introduction of additional shear strain through the thickness of ASR rolled sheets would be beneficial to the grain refinement.

## Acknowledgments

## References

1. K.H. Kim and D.N. Lee, "Analysis of deformation textures of asymmetrically rolled aluminum sheets," Acta Mater, 49 (2001)，2583-2595.

2. W.J. Kim et al., "Effect of the speed ratio on grain refinement and texture development in pure Ti during differential speed rolling," Scripta Mater, 64 (2011), 49-52.

3. W.J. Kim, S.J. Yoo and J.B. Lee, "Microstructure and mechanical properties of pure Ti processed by high-ratio differential speed rolling at room temperature," Scripta Mater, 62 (2010), 451-454.

4. W.Y. Kim and W.J. Kim, "Fabrication of ultrafine-grained Mg–3Al–1Zn magnesium alloy sheets using a continuous high-ratio differential speed rolling technique," Materials Science and Engineering: A, 594 (2014), 189-192.

5. J. Cho et al., "Texture and microstructure evolution during the symmetric and asymmetric rolling of AZ31B magnesium alloys," Materials Science and Engineering: A, 566 (2013), 40-46.

6. W.J. Kim, J.D. Park and W.Y. Kim, "Effect of differential speed rolling on microstructure and mechanical properties of an AZ91 magnesium alloy," Journal of Alloys and Compounds, 460 (2008), 289-293.

7. W.J. Kim et al., "Microstructure and mechanical properties of Mg–Al–Zn alloy sheets severely deformed by asymmetrical rolling," Scripta Material, 56 (2007), 309-312.

8. S. Kim et al., "Texture and microstructure changes in asymmetrically hot rolled AZ31 magnesium alloy sheets," Material Letter, 59 (2005), 3876-3880.

9. Y. Ding, J. Jiang and A. Shan, "Microstructures and mechanical properties of commercial purity iron processed by asymmetric rolling," Materials Science and Engineering: A, 509 (2009), 76-80.

10. Loorentz and Y.G. Ko, "Effect of differential speed rolling strain on microstructure and mechanical properties of nanostructured 5052 Al alloy," Journal of Alloys and Compounds," 586, Supplement 1(2014) S205-S209.

11. Loorentz and Y.G. Ko, "Microstructure evolution and mechanical properties of severely deformed Al alloy processed by differential speed rolling," Journal of Alloys Compounds, 536, Supplement 1(2012), S122-S125.

12. L.L. Chang, S.B. Kang and J.H. Cho, "Influence of strain path on the microstructure evolution and mechanical properties in AM31 magnesium alloy sheets processed by differential speed rolling," Mater Design, 44 (2013), 144-148.

13. Y.H. Ji, J.J. Park and W.J. Kim, "Finite element analysis of severe deformation in Mg–3Al–1Zn sheets through differential-speed rolling with a high speed ratio," Materials Science and Engineering: A, 454–455 (2007), 570-574.

14. Y.H. Ji and J.J. Park, "Development of severe plastic deformation by various asymmetric rolling processes," Materials Science and Engineering: A, 499 (2009), 14-17.

15.T. Inoue and N. Tsuji, "Quantification of strain in accumulative roll-bonding under unlubricated condition by finite element analysis," Computational Materials Science, 46 (2009), 261-266.

16. M.S. Chun and J.G. Lenard, "Hot rolling of an aluminum alloy using oil/water emulsions," Journal of Materials Processing Technology, 72 (1997), 283-292.

17. G.Y. LIN et al., "Flow stress of 7075 aluminum alloy during hot compression deformation," The Chinese Journal of Nonferrous metals, 3 (2001), 412-415.

18. H. Watanabe, T. Mukai and K. Ishikawa, "Differential speed rolling of an AZ31 magnesium alloy and the resulting mechanical properties," Journal of Materials and Science, 39 (2004), 1477-1480.

19. Q. Cui and K. Ohori, "Grain refinement of high purity aluminium by asymmetric rolling," Materials Science and Technology, 16 (2000), 1095-1101.

20. K.Y.Y.S. T. Sakai, "Control of through-thickness shear texture by asymmetric rolling," Materials Science Forum, 396-402 (2002), 309-314.

21. N. Kamikawa, T. Sakai and N. Tsuji, "Effect of redundant shear strain on microstructure and texture evolution during accumulative roll-bonding in ultralow carbon IF steel," Acta Mater, 55 (2007), 5873-5888.

22. F. Zuo et al., "Shear deformation and grain refinement in pure Al by asymmetric rolling," Transactions of Nonferrous Metals Society of China, 18 (2008), 774-777.

23. S.H. Lee et al., "Role of shear strain in ultra-grain refinement by accumulative roll-bonding (ARB) process," Scripta Mater, 46 (2002), 281-285.